Acta Phys. Hung. A 21/2–4 (2004) 237–242

HEAVY ION
PHYSICS

Elliptic Flow Measurements from STAR

Raimond Snellings[1] for the STAR Collaboration

[1] NIKHEF, Kruislaan 409, 1098 SJ Amsterdam, The Netherlands
E-mail: Raimond.Snellings@nikhef.nl

Received 13 June 2003

Abstract. In these proceedings some of the highlights of the elliptic flow measurements from STAR at $\sqrt{s_{NN}} = 130$ and 200 GeV for Au+Au collisions are presented.

Keywords: relativistic heavy-ion collisions, collective flow, quark–gluon plasma
PACS: 25.75.Ld

1. Introduction

Elliptic flow characterizes the anisotropy in particle emission "in" and "out" of the reaction plane. The word flow is used to describe collective behavior but does not necessarily imply a hydrodynamic interpretation. Elliptic flow is commonly characterized by the second harmonic coefficient v_2 of an azimuthal Fourier decomposition of the particle momentum distribution versus the reaction plane.

Based on general arguments it is thought that elliptic flow develops mostly in the first few fm/c ($<$ radius of the nucleus) and thus provides information about the amount of thermalization achieved *early* in the collision. In fact, the observed elliptic flow for charged and identified particles at RHIC is interpreted as:

- one needs very strong interactions between the quarks and gluons at very early times in the collision [1],
- a well-developed quark–gluon plasma [2].

2. Integrated Elliptic Flow and Non-Flow Contributions

Experimentally the reaction plane is not known, and elliptic flow is often reconstructed from two-particle azimuthal correlations. Two-particle azimuthal correlations can be affected by many other sources besides elliptic flow. These so called non-flow effects could be large [3] and this would change the interpretation of strong re-interactions of the constituents early in the collision. STAR has estimated the contribution of non-flow in the first elliptic flow paper from RHIC [4]. Figure 1 taken

1219-7580/04/ $ 20.00

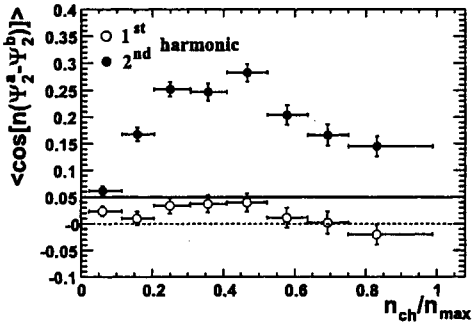

Fig. 1. Correlation between the event plane angles determined from two independent subevents for the first and second harmonic

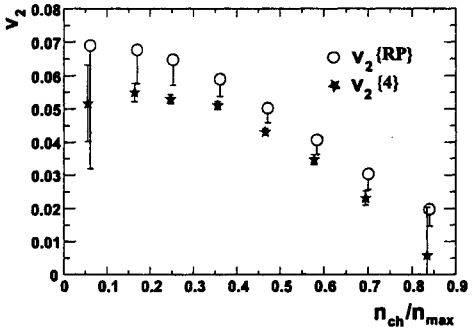

Fig. 2. Identified particle elliptic flow versus centrality from the reaction plane, $v_2\{\mathrm{RP}\}$, and the four particle cumulant, $v_2\{4\}$, method

from [4] shows the correlation between two event plane angles for two independent subevents for the first and second harmonic as a function of centrality. In the case of flow the correlation of the second harmonic event plane angles will be proportional to $M \cdot v_2^2$, where M is the multiplicity of particles used in the determination of the event plane. The observed peaked shaped as a function of centrality is characteristic of elliptic flow. This peaked shape originates from the fact that M increases as a function of centrality while elliptic flow decreases. Every model description of a heavy-ion collision which includes final state interactions will yield such a shape, the magnitude and peak position as a function of centrality will depend on the amount of re-interactions. Non-flow contributions will be monotonic or almost constant for this quantity, which is also true in the specific case of non-flow due to mini-jets as calculated in [3]. Based on this correlation the estimated maximum non-flow contribution, taken constant as a function of centrality, was 0.05. The propagation of this estimate to the measured v_2 values is shown in Fig. 2. In this figure the v_2 values versus centrality are shown as open circles and the asymmetric uncertainties are the non-flow estimates [6].

More recently a new analysis method based on cumulants was proposed [7] which utilizes the fact that true flow is a multi-particle correlation. The obtained elliptic flow values using this method for four particle correlations, $v_2\{4\}$, is also shown in Fig. 2 as solid stars. A detailed description of the cumulant analysis in STAR for the $\sqrt{s_{NN}} = 130$ GeV data is given in Ref. [8]. The reduction in the integrated elliptic flow between the two methods shows the (possible) contribution of non-flow effects at this energy. There are, however, two important caveats associated with calculating v_2 using two or multi-particle correlations. First the four particle cumulant is reliable when the magnitude of $v_2\{4\} > 1/N^{3/4}$ [7, 3], where N is the number of "clusters" contributing to the measurement. However, this is an important improvement over the two particle analysis which is reliable when $v_2\{2\}$

$> 1/N^{1/2}$. Secondly, event by event fluctuations could affect $v_2\{2\}$ differently than $v_2\{4\}$. The two particle analysis is sensitive to v_2^2 while the four particle cumulant analysis is sensitive to the difference between v_2^4 and v_2^2. The v_2 value is obtained by averaging over events and due to event by event fluctuations in general $\langle v_2 \rangle^2 \neq \langle v_2^2 \rangle$ and $\langle v_2 \rangle^4 \neq \langle v_2^4 \rangle$. This can also lead to a reduction in the v_2 obtained from the four particle compared to the two particle correlation methods [8,9].

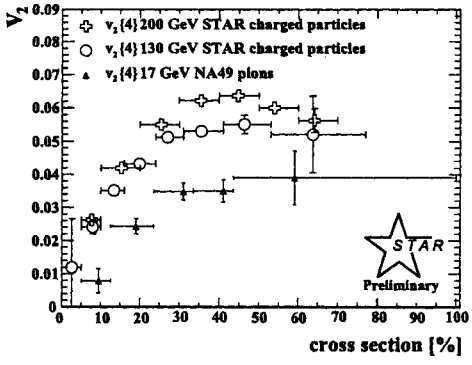

Fig. 3. Centrality dependence of elliptic flow for collisions at $\sqrt{s_{NN}}$ = 17, 130 and 200 GeV

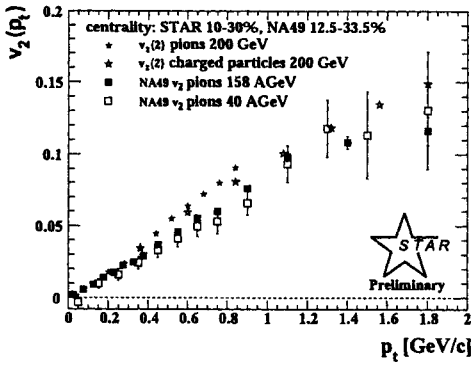

Fig. 4. Comparison of $v_2(p_t)$ for SPS and RHIC energies

Even with these caveats, the most reliable way of calculating v_2 when the reaction plane is not known is via a higher order cumulant method. Figure 3 shows the measured $v_2\{4\}$ values as a function of centrality for $\sqrt{s_{NN}}$ = 130 and 200 GeV. The elliptic flow as a function of centrality for both energies is very similar. The maximum difference is about 20%, however, note that only the statistical uncertainties are shown. For the preliminary 200 GeV results the systematic uncertainties are also about 20%. Also shown are the measurements from NA49 at the CERN SPS. The increase in the integrated elliptic flow between SPS and RHIC energies can be caused by an increase in the mean transverse momentum or due to a higher slope of the differential $v_2(p_t)$ [9]. Figure 4 shows the differential $v_2(p_t)$ for SPS and RHIC energies. While the slope increases, which indicates the increase in elliptic flow at RHIC, the dominant contribution to the integrated elliptic flow comes from the value of v_2 around mean p_t of the particles. In the p_t range of 350–500 MeV/c, the $v_2(p_t)$ values at SPS and RHIC energies are very close. However, the mean p_t difference between pions at the SPS and charged particles at RHIC is about 150 MeV/c which already accounts for most of the difference in integrated v_2.

3. Elliptic Flow for Identified Particles

The elliptic flow as a function of transverse momentum, $v_2(p_t)$, depends on the temperature, radial flow velocity, azimuthal variation of the transverse flow veloc-

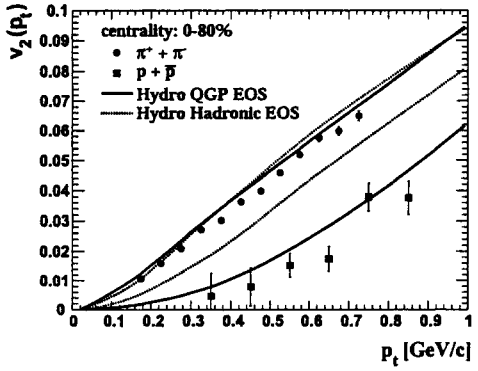

Fig. 5. $v_2(p_t)$ for pions and protons at $\sqrt{s_{NN}} = 130$ GeV. The lines are hydrodynamical model calculations.

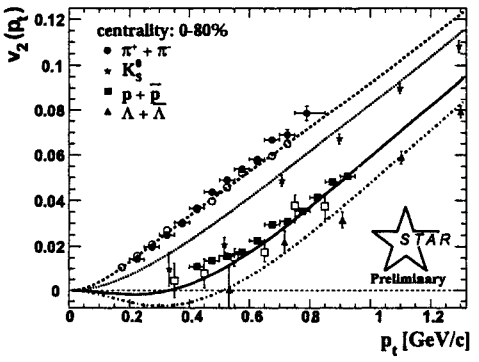

Fig. 6. Comparison of $v_2(p_t)$ for identified particles at $\sqrt{s_{NN}} = 130$ and 200 GeV Au+Au collisions

ity and the spatial anisotropy of the system at freeze-out [10]. The measurement of $v_2(p_t)$ for different particle masses constrains these parameters with reasonable precision [10]. These freeze-out parameters in combination with the initial conditions strongly constrain the Equation Of State (EOS). In Fig. 5 the measured $v_2\{2\}$ versus p_t at $\sqrt{s_{NN}} = 130$ GeV for pions and protons + antiprotons is shown [10] together with hydrodynamical model predictions [11] for two different EOS. This clearly illustrates that the heavier particles are more sensitive to the underlying EOS. This can be understood from the fact that the lighter particles are very sensitive to the freeze-out temperature while the heavier particles more directly reflect the flow. From Fig. 5 it is clear that for these model calculations the data prefer the quark–gluon plasma EOS. Figure 6 shows in solid symbols the $v_2\{2\}$ versus p_t for pions, K^0_S's, protons + antiprotons and $\Lambda + \bar{\Lambda}$ at $\sqrt{s_{NN}} = 200$ GeV. For comparison the $v_2(p_t)$ for pions and protons + antiprotons at $\sqrt{s_{NN}} = 130$ GeV in open symbols are included. The lines shown are the results from the blastwave fits to the $\sqrt{s_{NN}} = 130$ GeV data [10]. From this comparison it is clear that the $v_2(p_t)$ for different particles at these different energies is very similar. The pions do show, however, a slightly higher slope at $\sqrt{s_{NN}} = 200$ GeV.

4. Elliptic Flow at Intermediate Transverse Momentum

Elliptic flow measurements can quantify the possible modifications of the created medium on the particle yields as a function of p_t. A medium modification like the predicted mechanism of parton energy loss, jet quenching, will inevitably lead to a finite v_2 at high p_t.

Figure 7 shows the measured $v_2(p_t)$ up to 7 GeV/c obtained by two, $v_2\{2\}$ and $v_2\{\mathrm{RP}\}$, and four, $v_2\{4\}$, particle correlation methods. The measurement of $v_2\{4\}$

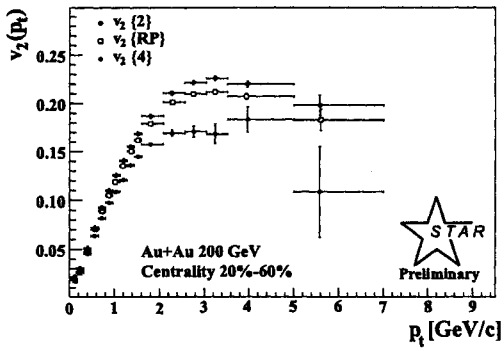

Fig. 7. Charged particle elliptic flow obtained by two ($v_2\{2\}$ and $v_2\{\mathrm{RP}\}$) and four ($v_2\{4\}$) particle correlation methods

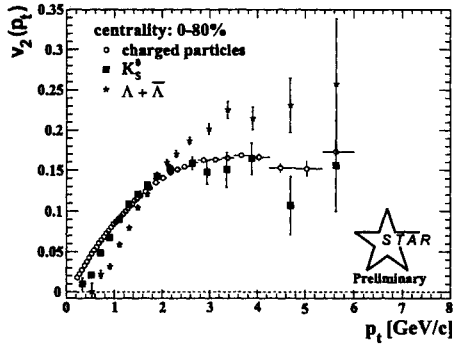

Fig. 8. Elliptic flow versus p_t for charged particles, $\Lambda + \bar{\Lambda}$ and K^0_S

shows that there is a significant amount of elliptic flow out to $p_t = 5$–6 GeV/c. The medium modification inferred from this observable in addition to the suppression of the single inclusive particle yield [12], characterized by R_{AA}, and the disappearance of high-p_t angular back-to-back correlations, as seen in the centrality dependence of I_{AA} [13], is in qualitative agreement with the predictions of jet quenching. At high p_t the measurement of R_{AA}, I_{AA} and v_2 for the different particle species can provide a better constraint on the underlying mechanism responsible for the modification of the particle yield. That R_{AA} depends on particle species was observed by PHENIX [14] for π^0's and charged particles. The comparison of the single inclusive particle yield for $\Lambda + \bar{\Lambda}$ and K^0_S in central and peripheral collisions as measured by STAR also shows this species dependence [15]. The suppression in the single inclusive particle yield at intermediate p_t for K^0_S is stronger than for $\Lambda + \bar{\Lambda}$. The measured $v_2\{2\}$, shown in Fig. 8, for $\Lambda + \bar{\Lambda}$ and K^0_S at the same intermediate p_t is also particle dependent. The $v_2(p_t)$ above 2 GeV/c for the $\Lambda + \bar{\Lambda}$ is larger than the $v_2(p_t)$ of K^0_S. It is assumed that the non-flow contributions in this measurement are approximately equal for both particle species and therefore the difference is a real difference in flow.

Explaining the origin of this suppression of single inclusive particle yield and elliptic flow for identified particles at intermediate p_t due to jet quenching alone seems not to work. To understand this observed behavior better a measurement of the contribution of the initial state Cronin effect in dA as well as a measurement of I_{AA} for $\Lambda + \bar{\Lambda}$ and for K^0_S is needed. Another possible explanation is that the hydro-like behavior extends further in p_t for $\Lambda + \bar{\Lambda}$ then for K^0_S.

Another puzzle is the rather large values of elliptic flow at intermediate p_t. The interpretation that this is caused by radiative energy loss or due to inelastic interactions in a parton cascade would lead to rather large initial parton densities. Corrections for non-flow would already reduce the elliptic flow values and therefore

the parton densities needed. In addition a mechanism like parton coalescence would require much smaller parton elliptic flow to account for the measured particle elliptic flow and would also explain the different v_2 values observed at intermediate p_t for $\Lambda + \bar{\Lambda}$ and K^0_S [16].

5. Conclusions

Large elliptic flow values have been measured by STAR both at $\sqrt{s_{NN}} = 130$ and 200 GeV Au+Au collisions. The large magnitude of the charged and identified particle elliptic flow at low p_t is interpreted as due to strong interactions between the partons at early times in collision and even approaches the ideal hydrodynamical limit. While non-flow is not negligible at higher p_t, elliptic flow extends at least up to 6 GeV/c. This unambiguously shows the effect of medium modification on the particle yield in this transverse momentum range. The dependence of the elliptic flow and the single particle inclusive yield on particle species at intermediate p_t shows that radiative energy loss can not be the only medium induced modification of the particle yield in this p_t range.

References

1. L. McLerran, hep-ph/0202025.
2. U. Heinz, hep-ph/0109006; E. Shuryak, nucl-th/0112042.
3. Y.V. Kovchegov and K.L. Tuchin, *Nucl. Phys.* **A708** (2002) 413.
4. K.H. Ackermann et al. (STAR Collaboration), *Phys. Rev. Lett.* **86** (2001) 402.
5. NA49 Collaboration, nucl-ex/0303001.
6. R.J.M. Snellings (STAR Collaboration), *Nucl. Phys.* **A698** (2002) 193c.
7. N. Borghini, P.M. Dinh, J.-Y. Ollitrault, *Phys. Rev. C* **64** (2001) 054901.
8. C. Adler et al. (STAR Collaboration), *Phys. Rev. C* **66** (2002) 034904.
9. S.A. Voloshin, *Quark Matter 2002*, nucl-ex/0210014.
10. C. Adler et al. (STAR Collaboration), *Phys. Rev. Lett.* **87** (2001) 182301.
11. P. Huovinen et al., *Phys. Lett.* **B500** (2001) 58.
12. J.C. Dunlop (STAR Collaboration), *19th Winter Workshop on Nuclear Dynamics*, eds. W. Bauer, R. Bellwied, J.W. Harris and G.D. Westfall, Breckenridge, Colorado, USA, February 8–15, 2003, *Acta Phys. Hung. A* **21** (2004) 215.
13. J.W. Harris (STAR Collaboration), *19th Winter Workshop on Nuclear Dynamics*, eds. W. Bauer, R. Bellwied, J.W. Harris and G.D. Westfall, Breckenridge, Colorado, USA, February 8–15, 2003, *Acta Phys. Hung. A* **21** (2004) 229.
14. PHENIX Collaboration, *Phys. Rev. Lett.* **88** (2002) 022301.
15. R. Belwied (STAR Collaboration), *19th Winter Workshop on Nuclear Dynamics*, eds. W. Bauer, R. Bellwied, J.W. Harris and G.D. Westfall, Breckenridge, Colorado, USA, February 8–15, 2003, *Acta Phys. Hung. A* **21** (2004) 199.
16. D. Molnar and S.A. Voloshin, nucl-th/0302014.